
Article:
Gallello, Gianni, Ramacciotti, Mirco, Lezzerini, Marco et al. (5 more authors) (2017) Indirect chronology method employing rare earth elements to identify Sagunto Castle mortar construction periods. Microchemical Journal. pp. 251-256. ISSN: 0026-265X

https://doi.org/10.1016/j.microc.2017.02.009

Indirect chronology method employing Rare Earth Elements to identify Sagunto Castle mortar construction periods

Gianni Gallello[*a] , Mirco Ramacciotti[a], Marco Lezzerini[bd], Emilia Hernandez[c] , Matias Calvo[c], Angel Morales[a], Agustin Pastor[a], Miguel de la Guardia[a]

[a]Department of Analytical Chemistry, University of Valencia, 50 Dr. Moliner Street, 46100 Burjassot, Valencia, Spain

[b]Department of Earth Sciences, University of Pisa, Via S. Maria 53, 56126 Pisa, Italy

[c]Sagunto Archaeological Museum 23 del Castillo Street, 46500 Sagunto, Valencia, Spain

[d]Applied and Laser Spectroscopy Lab., ICCOM-CNR, Via G. Moruzzi 1, 56124 Pisa, Italy

Abstract

A novel indirect chronology method has been developed to identify Sagunto Castle construction periods. The method is based on the use of inductively coupled plasma mass spectrometry (ICP-MS) to determine rare earth elements (REE) and other trace elements in mortars. Additionally, a no destructive geochemical analysis based on X-ray fluorescence (XRF) was employed for major elements determination. Collected chemical data were processed through Principal Component Analysis (PCA) to highlight any differences among the mortars belonging to different buildings and construction periods. The results show that PCA analysis permits to discriminate

construction periods according to mortar sample REE contents. Major elements and trace elements show just coarse differences related to the mortar composition. The proposed method permitted to clarify important issues about wall stratigraphy and its effectiveness on a novel indirect chronology developed method.

Keywords: Mortar, Rare Earth Elements (REE), ICP-MS, multivariate statistics, indirect chronology, Sagunto Castle.

*Corresponding author: Gianni Gallello

Tel.+34697636957

Fax+34 96 3544838

Email: gianni.gallello@] uv.es

1. Introduction

The study of ancient mortars is of pivotal importance to understand the building process of archaeological and architectural heritage. Mortar chemical analyses have been carried out to identify raw materials provenance [1,2], to know processing procedures [3,4,5] and also for restoration purposes [6,7,8]. For example, Marra et al. [2] performed geochemical and petrographic methods to characterize the different natural pozzolanic materials used in the ancient mortars of some Roman monuments and to determine their provenance. The study of mortars samples from Roman catacombs, allowed Sánchez-Moral et al. [8] to collect information about their setting techniques in relation to their function and to determine the state of conservation of mortars exposed to the particular conditions of hypogean environments. Moreover, data confirmed to be particularly useful to verify the

sequence of construction phases retraced by the archaeologists, and to solve chronological issues [9,10,11,12]. In particular, Arizio et al. [9], carried out statistical treatment of data obtained from calcimetric and chromatography analyses on the mortars of the Balivi Tower in Aosta (Italy) for distinguishing different construction phases on basis of chemical composition of the mortars.

Mineralogical and petrographic methods have often been employed to study ancient mortars. Thermogravimetric analysis (TGA) has been used especially to determine the hydraulic character of the binder fraction [13,14,15]. X-ray fluorescence (XRF), frequently associated with other techniques such as optical microscopy (OM), scanning electron microscopy (SEM) and X-ray diffraction (XRD), provided excellent methods to detect the main features of a mortar [16,17,18,19]. In a recent paper, Leone et al. [18] have used some of these techniques to characterize mortar samples from the Roman city of Herculaneum (Italy) and to determine their degradation state. In particular, they were able to determine the mortar conservation measuring porosity and aggregate/binder ratio by OM, and through the presence of sulphurous compounds detected by XRF and TGA.

In This work a pioneering archaeometric study was carried out on the famous Castle of Sagunto. Due to the uncertainty of the archaeological studies, carried out in a context characterized by a complex stratigraphy of the masonries, by a long and continuous occupation and by the reemployment of materials in different historical periods, for the first time an indirect chronology method, based on mortar rare earth elements (REE) analysis, has been developed to clarify issues concerning the building stratigraphy and construction phases of the monument.

The area of Sagunto (Valencia, Spain) has been occupied since the Iberian period, at least since the 5th century BC (See Figure 1). The importance of the city increased under the influence of Rome and in 218 BC it was destroyed by Hannibal after a long siege during the Second Punic War. After the war, the city of Sagunto became a Roman *municipium* and in the first Imperial Age it was interested by the construction of important buildings such as the theater [20], which was recently restored, and the anphitheatre. After the fall of the Roman Empire, Sagunto became part of the Visigothic Kingdom and then of the Caliphate of Cordoba until it was reconquered by James I of Aragon in the 13th AD during the *Reconquista,* after five centuries of Muslim Arab domination. More recently, Sagunto was the centre of an important battle between the French and the Spanish troops during the Napoleonic Wars (1811), in which the Castle suffered heavy damages. In the 20th century, the Castle of Sagunto was interested by important restoration works and was designed heritage of cultural interest by the Spanish authorities [21,22]. The archaeological park of Sagunto Castle has recently become one of the most important attractions for cultural tourism in Valencia region and in Spain.

Innovative methodological approaches employing REE have been recently established to tackle challenging archaeological problems related to the polished stone raw material origins [23] and soil formations [24,25]. REE and other trace elements analysis have been used by some authors to identify mortar raw materials [2,3,26,27,28]. For example, studies of REE in mortar samples were carried out by Mirello et al. [27] employing La/Ce ratio, to identify the provenance of limestone employed to made the mortars at the Aztec Sacred Precinct of Tenochtitlan (Mexico City).

The principal aim of this paper has been prove the effectiveness of REE to distinguish the intricate construction phases of Sagunto Castle and therefore to develop an indirect chronology method. Major elements, REE and other trace elements were determined on a total of 51 samples collected from different buildings of the studied archaeological heritage. Mineralogical and petrographic analyses were also carried out in some selected samples. The multi-element capability of Inductively Coupled Plasma Mass Spectromety (ICP-MS) was employed to measure REE and other trace elements. X-ray fluorescence (XRF) that permit direct, fast, cheap and safe chemical analyses was also employed to determine some major elements. Finally multivariate statistic employing Principal Components Analysis (PCA) was used to observe mortar samples distribution.

2. Materials and methods

2.1 The studied samples

Fifty-one samples were sampled from Sagunto Castle masonry (See Figure 1). In table 1 the macroscopic characteristics of the sampled mortars can be appreciated. Ten samples (S6, S7, S8 S41, S44, S59, S60, S61, S62 and S63) were collected from a wall considered a part of the Sagunto fortification during the Roman Republican period (SMR). Three samples (S47, S72 and S45) from a structure belonging to the Roman Republican *Forum* (FRW) located on the western area of the Castle and three (S54, S46 and S57) from the Temple (TMP) nearby the *Forum*. Seven samples (S12, S13, S14, S15, S16, S37 and S38) were collected from a tower included in the Muslim defensive wall, called *Torre Centrale Estudiantes* (TCE). According to the archaeological interpretations, TCE foundations have been dated

back to the republican period and it was characterized by other building interventions in the Islamic and modern periods [29]. Six samples were collected in the Roman Imperial Forum [30] area: two of them (S48 and S49) come from the *tabernae* (TFI) and five (S3, S50, S51, S55 and S58) from the basilica (FBI) where the sample S51 was collected from a wall considerate from an uncertain period. This last building was especially affected by different construction interventions during the Islamic occupation. Three other samples were collected from Imperial *Forum* in a structure identified as the *Curia* (CUR): two (S52 and S53) from the walls and one (S56) from the pavement. Six samples were collected from the Roman Theatre (TR): two samples (S64 and S65) from the foundations of the *proscaenium*, one sample from the *valva regia* (S67), another (S68) from the restored façade of the western *aditus* and two samples, (S66 and S69), from the *ima cavea* western area. Ten samples were collected from the Islamic Wall: four (S1, S17, S39 and S40) from the first track (MI) and five (S9, S10, S11, S42 and S43) from the second one (MII). However the archaeologists suspected that MII was rebuilt in the Modern Age due to the damages suffered during the Napoleonic Wars. Sample, S2 was collected from the 16th century Wall MXVI, and sample S4 from the 17th century Hermitage (ERM) being S5 taken from a Napoleonic barrack (DNAP).

2.2 Mineralogical and petrographic analysis

Mineralogical and petrographic analysis could be carried out just in well preserved mortars. The macroscopic features of some mortar samples (S1, S2, S3, S4 and S5) were observed with a Wild-M3C stereomicroscope up to 200 magnifications. Mineralogical and petrographic investigations of the mortar samples were performed by optical microscopy (OM) on polished thin sections using a Zeiss-Axioplane polarising

microscope. The grain sizes of the aggregate particles are reported according to the scheme proposed by the British Geological Survey based on the Wentworth scale. The quantitative mineralogical composition (volume percentages) of the mortar samples has been determined by modal analysis (no less than 200 points) performed on polished thin sections.

Qualitative mineralogical compositions of the mortars, enriched binders, aggregate fractions and lumps were performed by X-ray powder-diffraction (XRPD) by means of an automatic diffractometer Philips PW 1830/1710 in the following experimental conditions: Bragg-Brentano geometry, Ni-filtered CuKα radiation obtained at 40 kV and 20 mA, 5-60 °2θ investigated range, 0.02° step, 2 s counting time per step.

Scanning electron microscope observations and micro-chemical compositions of intergranular binder and lumps were performed using a Philips XL30 instrument equipped with an energy dispersive spectrometry EDAX (standardless software DXi4) with 20 kV acceleration voltage, 0.1 nA beam current, and 100 s live time.

2.3 XRF analysis

Homogenized and pestle samples were directly analysed by using a portable X-ray fluorescence. Instrument spectra were obtained using a portable model S1 Titan energy dispersive X-ray fluorescence spectrometer from Bruker (Kennewick,Washington DC, USA) equipped with a Rhodium X-ray tube and X-Flash® SDD detector. For instrument control S1RemoteCtrl (Geochem-trace programme) and S1Sync software from Bruker were employed to measure percentage of Al_2O_3, SiO_2, CaO, Ti, Fe and for spectra treatment, the ARTAX software from Bruker was used. The standard error of readings during the analysis ranged from 1% to 9% for oxides and elements. Reference standard soil NIM GBW07408 and lime stone NCS DC60108a were used as standard

reference materials for evaluating the quality of the employed method (Table 2). In case of lime stone NCS DC60108a, Ti levels are below the limit of detection and also the inadequate uncertainty of Al_2O_3 is related to the sensitivity of the employed device.

2.4 ICP-MS analysis

Sample preparation and digestion were carried out pre-crashing the mortar samples employing a jaw crusher, and an agate mortar.

The selected digestion method consisted in the addition of 1.35 ml HCl and 0.45 ml HNO_3(Using 37% HCL and 69% HNO_3 high purity stock bottles) to 0.15g of sample in glass tubes placing them in a water bath at 100°C for 40 min. Subsequently, the digested solutions were carefully poured into plastic tubes of 50 ml, bringing the volume to 25 ml with purified water. The solution was used to measure trace elements such as Ba, Bi, Cd, Cr, Co, Cu, Pb, Li, Mn, Mo, Ni, Sr, Tl, V, Zn and REEs (La, Ce, Pr, Nd, Sm, Eu, Gd, Tb, Dy, Ho, Er, Tm, Yb, Lu,) Sc and Y. A multi-element stock solution for ICP analysis in HNO_3 5%, containing the mentioned elements at a concentration of 100 µg/ml, was used to prepare the calibration standard. 5 ml volumetric flasks were used adding 0.15 ml of HNO_3, 0.45 ml of HCl and the corresponding volume of standard solution and filling up to volume with pure water. The prepared dilutions were analyzed by ICP-MS with Perkin Elmer Elan DRCII (Concord, Ontario, Canada). To avoid the obstruction of the nebulizer system samples were filtered employing filter paper (Whatman™ N.1 of 70mm). Concentration ranges between 1 and 600 µg/l were used for trace elements (Ba, Bi, Cd, Cr, Co, Cu, Pb, Li, Mn, Mo, Ni, Sr, Tl, V, Zn, La, Ce, Pr, Nd), and concentration ranges between 1 and 100 µg/l for Sm, Eu, Gd, Tb, Dy, Ho, Er, Tm, Yb, Lu. All standards were acquired from Sharlab S.L. (Barcelona). Soil NIM GBW07408 and limestone NCS DC60108a were

used as standard reference materials for evaluating the analytical quality of the method. Rh was used as internal standard for ICP-MS analyses.

Analyses were performed by ICP-MS employing the analytical parameters in Table 3. Thirty-one elements were analysed including major elements, trace elements and REE. The analytical mass isotope instrumental detection and quantification limits (LOD and LOQ, respectively) and R^2 are listed in Table 4.

2.5 Data analysis

For statistical analysis 51 samples were employed. All variables (major elements, REE and other trace elements) were used for modelling. PCA was used to explore large geochemical datasets reducing the number of variables and providing a deep insight into the structure of the variance of the dataset. For PCA analysis 51 samples and 36 variables, mean centering and autoscaling pre-processing prior to modelling were used. Cross validation was carried out employing leave one out method.

Data analysis was carried out using the PLS Toolbox 6.5 for Eigenvector Research Inc., (Wenatchee, WA, USA) running in Matlab R2014b from Mathworks Inc., (Natick, MA, USA).

3. Results and discussion

3.1 Mineralogical and petrographic features

From the petrographic point of view, the studied samples (S1, S2, S3, S4 and S5) are strongly inhomogeneous due to the presence of abundant lumps. The aggregate-binder ratio ranges from 3:1 to 1:3 in all samples (in some cases the sample is substantially a

lump of lime with little or no aggregate and other mortars with low aggregate to binder ratio). The binder mortars were obtained by baking an impure limestone and the binder fraction seems to consist of calcite + CSH phases (data not shown). Regarding the mineralogy of the aggregate could be observed the presence of clasts of quartz, feldspars, fragments of plutonic rocks and of carbonate rocks. It should be emphasized that the fragments of carbonate rocks are sometimes coarse and particularly abundant. The analysed samples seems to be very similar looking at the mineralogy and petrography, however the abundance of limestone fragments show that probably the limestone outcrops on the bases of the hill hosting Sagunto Castle were exploited to made the mortars for many centuries, as confirmed by the archaeological evidences, in fact the sample belong to the Roman Imperial period (S3), Islamic period (S1), XVI century (S2), XVII century (S4) and Napoleonic period (S5).

3.2 Major elements composition

Samples were measured by XRF and Figure 2 shows the spectra obtained for all the samples. Table 5 summarizes the concentration values expressed in percentage of Al_2O_3, SiO_2, CaO, Fe and Ti. Two groups could be clearly identified looking at CaO and SiO_2 levels. In fact, silica is the main compound of the samples belonging to SMR, FRW, TMP, most of TCE and one of CUR (S52) groups ranging between 51.2% and 32.1%, containing also low CaO levels from 22.7% to 13.2%. In the other sample groups (FBI, TFI, TR, MI, MII, MXVI, ERM, DNAP and some of TCE and CUR) the level of CaO was high, ranging between 35.0% and 52%, while SiO_2 content was low and ranged from 21.6% to 7.8%. The groups characterized by high silica levels contained also high values of Al_2O_3 (13.9% to 2.0%), Fe (2.8% to 2.0%) and Ti (0.3% to 0.2%).While sample S52 was characterized by high levels of silica and alumina, its concentrations of Ti (0.09%) and Fe (1.0%) were very low. The samples of the other

groups with CaO as the main compound are characterized by low levels of alumina (1.2% to 0.3%), Fe (1.7% to 0.7%) and Ti (0.2% to 0.06%).

3.3 REE and trace elements composition

As mentioned above samples were measured by ICP-MS and the results obtained are reported in Tables 6 being expressed the elemental concentration in μg/g. The obtained mean concentrations with their standard deviations show differences in geochemical composition in the studied groups. REE concentrations showed higher results in SMR (76 to 51 μg/g), TMP (76 to 64 μg/g), FRW (64to 43μg/g), MII (54to 45μg/g), DNAP (53μg/g) and TCE (56 to 43μg/g) although in this last group samples S12 (33 μg/g) and S14 (31 μg/g) show low REE levels. On the other hand, low REE levels are found in the remaining groups: CUR (31to 24 μg/g), FBI (30to 24μg/g), TFI (34 to 30μg/g), MI (36 to 25μg/g), ERM (33 μg/g), MXVI (35 μg/g) and TR (27 to 19μg/g). In this last group, sample S68 shows high levels of REE (46 μg/g). High concentrations of Y are found in SMR (9.63 to 6μg/g), FRW (11 to 8μg/g), TMP (11 to 8 μg/g), MII (7to 6 μg/g) and DNAP (8μg/g). In the other groups low values of REE are observed (MI, CUR, TFI, FBI, MXVI and ERM). S68 and S69, belonging to TR group, show high Y levels, which are 14μg/g and 8μg/g respectively, while the other samples (S64, S65, S66 and S67) got values between 6μg/g and 5μg/g. TCE presents higher values for S13, S15 and S16 (from 9μg/g to 8 μg/g) and low ones for S12, S14, S37 and S38 (from 6μg/g and 5 μg/g). Trace element values for Bi, Tl, Cd, Sc, Ni, Co, Cr, V and Li do not show clear differences between the studied groups. In case of lead (Pb) the values ranged from 86to 7μg/g. However sample S45 belonging to the FRW group, shows anomalous values of Pb (263μg/g). Barium (Ba) concentrations are from 161 μg/g to 49μg/g and Mn are

between 778 and 172 but S68 (TR) has high values of both Ba (411μg/g) and Mn (2453 μg/g). Mo concentrations between the groups varied from 3 μg/g to 0.20 μg/g except for S60 (SMR) which value is particularly low (0.03 μg/g). Sr values are from 731 to 200, but S69 (TR) got high values (1391 μg/g). Finally copper (Cu) levels are between 60 μg/g and 4μg/g, except for S56 (CUR) with a value of 186 μg/g. Higher or lower trace elements values in some samples more than others are probably due to unintelligible causes so it is unlikely find an explication about that.

In short, results show that trace elements do not allow clearly discriminate samples from different groups. However, REE and Y put in evidence geochemical differences between mortars collected from differences structures of Sagunto Castle.

3.4 PCA study

Principal Component analyses (PCA) has been applied to the whole set of samples employing major-trace elements (See Figure 3) and REE (See Figure 4) as variables.

PCA of major compounds and trace elements (See Figure 3a) shows just a division of most samples in two groups, where the first two principal components explains the main part of the variance of data PC1 (40.36%) and PC2 (13.31%) respectively. Magnitude and signs of the *loadings* from PC1 indicate that the samples plotted in the right area of the graph are the richest in silica, alumina, Fe and Ti and the ones plotted in the left area are the richest in CaO (See Figure 3b).

Figure 4a shows the score plots of 51 mortar samples using REE. The first two principal components explain the main part of the variance of data PC1 (85.36%) and PC2 (8.38%) respectively. Score plots represented as data points (samples) projected into the PC space. In the scores plot it can be observed that the group of samples from the

Republican Roman Wall (SMR) are similar to the temple of Diana samples (TMP) and to the Republican forum group (FRW). SMR and TMP are differently distributed from the Islamic 2nd track wall group (MII) that is related to the Napoleonic barrack (DNAP). On the other hand Islamic wall 1st track samples (MI) are similar to the Basilica group (FBI), the tabernae (TFI), the curia (CUR), the Hermitage (ERM) and the XVI century wall (MXVI). The Theatre group (TR) appears homogeneous and different than the other groups except in case of sample S68 collected from a restored façade of the *aditus*. The Torre Central Estudiante samples are distributed between different groups. S13, S15 and S16 are similar to SMR, TMP and FRW groups. S37 and S38 are similar to MII and DNAP. Finally S14 and S12 samples are close to MI, FBI, TFI, CUR, ERM and MXVI groups. The PC distribution put on evidence clear differences between the structures belonging to the Roman Republican period, the Imperial period, the Islamic and modern periods and furthermore it is possible to observe as the structures reemployed by the different civilizations are located with one or another period depending of their REE composition.

In the plot shown in Figure 4b, it can be seen the contribution of the variables (elements) to the PC1, being the absolute intensity of the loading of each variable directly correlated with its contribution to the model and the sign with its direction. As explained above, PC1 contains useful information for differentiate mortar samples proceeding from different buildings. Magnitude and signs of the loading from PC1 clearly show that La, Ce, Pr, Nd, Sm, Eu, Gd, Tb, Dy, Ho, Er, Tm, Yb, Lu and Sc are the most important variables for model building and higher REE values could be appreciated in SMR, TMP and FRW groups that were collected in Roman Republican construction phases (See Table 1). On the other hand it can be concluded that Y is not a representative variable in the PCA model.

Resuming, the results show that REE analysis enable to distinguish between different construction periods and also allowed to observe material recycle from prior construction periods.

3.5 Evaluation of Sagunto Castle construction phases

The occupation of the Sagunto Castle area had been incessant for about two millenniums during which battles and devastations have come in succession, followed by several interventions of construction, rebuilding and restoration, frequently made by reemploying old materials. While these intricate sequences of events make the retracing of the different construction phases particularly hard for archaeologists, REE data and statistical treatments could provide an essential support in this task.

The mineralogical and petrographic study do not help to distinguish from construction phases but may show that for many century the row materials employed to made mortar were extracted from the limestones outcrops nearby the Castle.

Major and trace elements PCA analysis (See Figure 3) show the formation of two big groups. Those groups correspond almost exactly with the masonries dated back to the republican period and to the ones of the following phases respectively. Although it is uncertain that the aforementioned diversity could be caused by different state of conservation of the mortars, by their initial compositions or by both features. Samples S68 and S69 both from TR class do not fall in neither of the two groups and may be affected in their major compounds by Imperial Theatre recent restoration works. While the separation between the two big groups of evaluated is indeed a first step in the explanation of the relationship between mineral composition of masonries and

construction phases, the results do not allow us to go further in this task due to the unintelligible distribution of the studied structures.

On the other hand, the statistical results of REE permit to go deeper in this clarification of constructive phases (See Figure 4) allowing us to propose an innovative indirect chronology method and make considerations about the conservation state of the mortars (See Figure 5). The samples belonging to the republican *forum* (FRW), to the republican wall (SMR) and to the temple (TMP) are placed in a wide area which is mainly located in the right-down quarter of the graph. The dispersive distribution of the Republican period samples is probably due to the environmental effects. In fact, looking at the REE contents, S60, S59, S61, S62, S63, S57, S54 and S72 seem more affected by the environmental impact.

The single building that belongs certainly to the imperial period is the Theatre (TR) and its samples are plotted very close to each other, except for S68 that belongs to a recent restoration work. Samples S56 is similar to the TR mortars and it is in good agreement with the dating of the Curia (CUR). As regards the Muslim phase, three of the samples (S1, S39 and S40) from the first track of the Islamic wall (MI) have similar features as shown by the graph. The intermediate position of samples from FBI (S3, S50, S51, S55 and S58), CUR (S52 and S53) and that of S14 from *Torre Centrale Estudiantes* (TCE) does not allow to reach definitive conclusions. However their proximity to samples of MI and the archaeological data about the heavy reemployment of the Imperial *forum* area during the Islamic phase suggest their belonging to this period (especially S51 already considered from an uncertain period). Moreover, S3 (FBI) and S14 (TCE) were interpreted by the archaeologists as Muslim makeover. The chemical features of the *tabernae* (TFI) lean towards the same conclusions. The rest of samples of this graph area belongs to the TCE (S12), to a wall of the 16th century (S2) and to the Hermitage

of the century 17th (S4); while their position in the graph seem to confirm the modern dating of the three samples, their closeness to the Islamic phase samples suggest also the possibility of a modern reuse of Islamic buildings or, at least the processing of the same raw materials. The samples coming from the second track of a wall, considered by the archaeologists from the Islamic period (MII), have definitely a different composition than the others from the Muslim period. This fact could be explained by supposing the presence of two different construction phases during this period, although their semblance to the sample from the barrack of the 19th century and its possible reconstruction after the Battle of Sagunto during the Napoleonic Wars suggest a later attribution.

TCE samples distribution need a particular consideration. As previously mentioned, TCE tour foundations have been dated back to the Iberian-Roman period and it was reemployed in the Islamic and modern periods. If we have a look at figure 4 we can observe that the wall stratigraphy and chronology of this structure it is revealed by REE data. In fact S13, S15 and S16 could be part of the Roman republican period, S14 and S12 to the Muslim employed materials and ultimately S37 and S38 should belong to the Modern age.

Thanks to the capability of REE mortar analyses to discern the different occupation periods and to understand the wall chronology, significant advances have been reached on the study of an important monument as it is the Sagunto Castle.

4. Conclusions

The pioneering study carried out on Sagunto Castle mortars has revealed interesting data about the construction phases.

The statistical treatment of major compounds and trace elements data permitted to divide the mortars in two main groups: the first group is basically composed by mortars characterized by low levels of CaO and correspond to buildings and walls of the Republican period. The second group, including mortars characterized by high levels of CaO and that corresponds to buildings and walls of the following periods. This difference can be caused by both, the conservation state of the mortars and their initial composition. However, mineralogical and petrographic results together with archaeological evidences suggest that row materials employed to made mortar were extracted on the limestones outcrops nearby the Castle at least since the Imperial Roman Period until the modern times.

REE statistical analysis improves the aforementioned classification by finding additional subgroups and permitting to identify the different phases that followed the Republican period. In particular, the REE, levels of the mortars from the Imperial Theatre and from the first track of the Muslim Wall point out the influence of the Islamic construction phase on the buildings of the Imperial Forum area, which fall between these two phases. The mortars collected from the walls of the first Modern Age constitute a coherent group too, among the samples of the Islamic phase. The mortars from the wall of the second track of the Islamic Wall show a certain affinity with the sample from the Napoleonic barrack and it supports the theory of a reconstruction due to the damages suffered during the Napoleonic Wars.

In conclusion, the study of the mortars from the Castle of Sagunto permitted to clarify important issues about the wall stratigraphy of the archaeological site and the effectiveness of a novel indirect chronology developed method based on REE analysis was proven. Further studies will employ this novel methodological proposal to shed

light about the wall stratigraphy history of other important architectural heritage worldwide.

Acknowledgements

Authors acknowledge the financial support of Generalitat Valenciana (PROMETEO project II/2014/077) and Ministerio de Economia y Competitividad-Feder (Project CTQ 2014-52841-P and Project CTQ 2012-38635).

The authors would like to thanks all the students of Chemistry and Archaeology which have contributed to the realization of this study.

References

[1] D'Ambrosio E., Marra F., Cavallo A., Gaeta M., Ventura G., Provenance materials for Vitruvius' harenae fossiciae and pulvis puteolanis: Geochemical signature and historical-archaeological implications, J. Archaeol. Sci.: Rep. 2 (2015) 186–203.

[2] Marra F., Danti A., Gaeta M., The volcanic aggregate of ancient Roman mortars from the Capitoline Hill: Petrographic criteria for identification of Rome's "pozzolans" and historical implications, J. Volcanol. Geotherm. Res. 308 (2015) 113–126.

[3] Belfiore C.M., Fichera G.V., La Russa M.F., Pezzino A., Ruffolo S.A., Galli G., Barca D., A multidisciplinary approach for the archaeometric study of pozzolanic aggregate in Roman mortars: the case of *Villa dei Quintili* (Rome, Italy), Archaeom. 57 (2015) 269–296.

[4] Drdácký M., Fratini F., Frankeová D., Slížková Z., The Roman mortars used in the construction of the Ponte di Augusto (Narni, Italy) – A comprehensive assessment, Constr. Build. Mater. 38 (2013) 1117–1128.

[5] Franzini M., Leoni L., Lezzerini M., Sartori F., The mortar of the "Leaning Tower" of Pisa: the product of a medieval technique for preparing high-strength mortars, Eur. J. Mineral., 12 (2000) 1151-1163.

[6] Borges C., Santos Silva A., Veiga R., Durability of ancient lime mortars in humid environment, Constr. Build. Mater. 66 (2014) 606–620.

[7] Miriello D., Lezzerini M., Chiaravalloti F., Bloise A., Apollaro C., Crisci G.M., Replicating the chemical composition of the binder for restoration of historic mortars as an optimization problem, Comp. and Concr. 12 (2013) 553-563.

[8] Sánchez-Moral S., Luque L., Cañaveras J.C., Soler V., Garcia-Guinea G., Aparicio A., Lime pozzolana mortars in Roman catacombs: composition, structures and restoration, Cem. Concr. Res. 35 (2005) 1555–1565.

[9] Arizio E., Piazza R., Cairns W.R.L., Appollonia L., Botteon A., Statistical analysis on ancient mortars: A case study of the Balivi Tower in Aosta (Italy), Constr. Build. Mater. 47 (2013) 1309–1316.

[10] Bertolini L., Carsana M., Gastaldi M., Lollini F., Redaelli E., Binder Characterisation of mortars used at different ages in the San Lorenzo church in Milan, Mater. Charact. 80 (2013) 9–20.

[11] Cardoso I., Macedo M.F., Vermeulen F., Corsi C., Santos Silva A., Rosado L., Candeias A., Mirao J., A Multidisciplinary approach to the study of archaeological mortars from the town of *Ammaia* in the Roman province of Lusitania (Portugal), Archaeom. 56 (2014) 1–24.

[12] Corti C., Rampazzi L., Bugini R., Sansonetti A., Biraghi M., Castelletti L., Nobile I., Orsenigo C., Thermal analysis and archaeological chronology: The ancient mortars of the site of Baradello (Como, Italy), Thermochim. Acta 572 (2013) 71–84.

[13] Lezzerini M., Legnaioli S., Lorenzetti G., Palleschi V., Tamponi M., Characterization of historical mortars from the bell tower of St. Nicholas church (Pisa, Italy), Constr. Build. Mater. 69 (2014) 203–212.

[14] Moropoulou A., Bakolas A., Bisbikou K,. Characterization of ancient, byzantine and later historic mortars by thermal and X-ray diffraction techniques, Thermochim. Acta 269 (1995) 779–795.

[15] Moropoulou A., Bakolas A., Bisbikou K., Investigation of the technology of historic mortars, J. Cult. Herit. 1 (2000) 45–58.

[16] Ahmad Bany Yaseen I., Al-Amoush H., Al-Farajat M., Mayyas A., Petrography and mineralogy of Roman mortars from buildings of the ancient city of Jerash, Jordan, Constr. Build. Mater. 38 (2013) 465–471.

[17] Garofano I., Robador M.D., Duran A., Materials Characteristics of Roman and Arabic mortars and stuccoes from the *Patio de Banderas* in the Real Alcazar of Seville (Spain), Archaeom. 56 (2014) 541–561.

[18] Leone G., De Vita A., Magnani A., Rossi C., Characterization of archaeological mortars from Herculaneum, Thermochim. Acta 624 (2016) 86–94.

[19] Theodoridou M., Ioannou I., Philokyprou M., New evidence of early use of artificial pozzolanic material in mortars, J. Archaeol. Sci. 40 (2013) 3263–3269.

[20] Hernández E., El Teatro Romano de Sagunto, Valencia: Generalitat Valenciana; (1988).

[21] Monserrat J.M.M., Dos siglos de destrucción de Patrimonio Histórico de Sagunto (1807-2007), Arse 41 (2007) 231–262.

[22] Ripollés PP., Opulentissima Saguntum, Sagunto: Bancaja (2004).

[23] Gallello G., Orozco T., Pastor A., De la Guardia M., Bernabeu J., Regional Provenance of Dolerite Prehistoric Objects through Mineral Analysis, Microchem. J. 124 (2016) 167–174.

[24] Gallello G., Pastor A., Diez A., Bernabeu J., Lanthanides revealing anthropogenic impact within a stratigraphic sequence, J. Archaeol. (2014) doi: 10.1155/2014/767085.

[25] Gallello G., Pastor A., Diez A., La Roca N., Bernabeu J., Anthropogenic units fingerprinted by REE in archaeological stratigraphy: Mas d'Is (Spain) case, J. Archaeol. Sci. 40 (2013) 799–809.

[26] Fichera G.V., Belfiore C.M., La Russa M.F., Ruffolo S.A., Barca D., Frontoni R., Galli G., Pezzino A.; Limestone Provenance in Roman Lime-Volcanic Ash Mortars from the Villa dei Quintili, Rome. Geoarch. 30 (2015) 70–99.

[27] Miriello D., Barca D., Pecci A., De Luca R., Crisci G.M., López Luján L., Barba L., Plasters from different buildings of the sacred precinct of Tenochtitlan (Mexico City): characterization and provenance, Archaeom. 57 (2015) 100–127.

[28] Ortega L.A., Zuluaga M.C., Alonso-Olazabal A., Geochemical characterization of archaeological lime mortars: provenance inputs, Archaeom. 50 (2008) 387–508.

[29] Pascual Buyé I., Aranegui C., Una torre defensiva de época romano-republicana en el Castell de Sagunt, Saguntum 26 (1993) 189–203.

[30] Aranegui Gascó C., Hernández E., López Piñol M., El foro de Saguntum: la planta arquitectónica, Los foros romanos de las provincias occidentales, Ministerio de Cultural, Madrid (1987) 73-97.

FIGURE CAPTIONS

Figure 1. Map of Sagunto Castle and location of the sampling points. Pictures: a) Torre Central Estudiantes; b) a wall of the Basilica; c) the Roman Theatre; d) details of the 16th century Wall (foreground) and of the Islamic first track Wall (background).

Figure 2. PXRF spectra and measurement procedure (see inserted picture)

Figure 3. PCA study employing major elements and trace elements as variables. Scores (a) and loadings (b) plot of PC1.

Figure 4. PCA study of mortar samples employing REE, Sc and Y as variables. Scores (a) and loadings (b) plot of PC1.

Figure 5. PCA study of mortar samples employing REE vs proposed Indirect Chronology Model for sample taken at Sagunto Castle.

Sample	Location	Acronym	Age	Function	Type of mortar	Grain size1		Color		Cohesion2
						max dim.	of the aggregate	binder	aggegate	
S63	Republican wall	SMR	I-II BC	Masonry mortar	Joint mortar		sand	beige/brown	grey	Inc
S7	Republican wall	SMR	I-II BC	Masonry mortar	Joint mortar		sand	beige/brown	grey	Inc
S60	Republican wall	SMR	I-II BC	Masonry mortar	Joint mortar		sand	beige/brown	grey	Inc
S62	Republican wall	SMR	I-II BC	Masonry mortar	Joint mortar		sand	beige/brown	grey	Inc
S41	Republican wall	SMR	I-II BC	Masonry mortar	Joint mortar		sand	beige/brown	grey	Inc
S6	Republican wall	SMR	I-II BC	Masonry mortar	Joint mortar		sand	beige/brown	grey	Inc
S44	Republican wall	SMR	I-II BC	Masonry mortar	Joint mortar		sand	beige/brown	grey	Inc
S8	Republican wall	SMR	I-II BC	Masonry mortar	Joint mortar		sand	beige/brown	grey	Inc
S61	Republican wall	SMR	I-II BC	Masonry mortar	Joint mortar		sand	beige/brown	grey	Inc
S59	Republican wall	SMR	I-II BC	Masonry mortar	Joint mortar		sand	beige/brown	grey	Inc
S37	Torre Central Estudiantes	TCE	?	Masonry mortar	Joint mortar		sand	white/beige	grey	Inc
S13	Torre Central Estudiantes	TCE	?	Masonry mortar	Joint mortar		sand	white/beige	grey	Inc
S16	Torre Central Estudiantes	TCE	?	Masonry mortar	Joint mortar		sand	white/beige	grey	Inc
S15	Torre Central Estudiantes	TCE	?	Masonry mortar	Joint mortar		sand	white/beige	grey	Inc
S38	Torre Central Estudiantes	TCE	?	Masonry mortar	Joint mortar		sand	white/beige	grey	Inc
S14	Torre Central Estudiantes	TCE	?	Masonry mortar	Joint mortar		sand	white/beige	grey	Inc
S12	Torre Central Estudiantes	TCE	?	Masonry mortar	Joint mortar		sand	white/beige	grey	Inc
S72	Republican forum	FRW	I-II BC	Masonry mortar	Joint mortar		sand	beige/brown	grey	Inc
S47	Republican forum	FRW	I-II BC	Masonry mortar	Joint mortar		sand	beige/brown	grey	Inc
S45	Republican forum	FRW	I-II BC	Masonry mortar	Joint mortar		sand	beige/brown	grey	Inc
S54	Republican Diana's Temple	TMP	I-II BC	Masonry mortar	Joint mortar		sand	beige/brown	grey	Inc
S46	Republican Diana's Temple	TMP	I-II BC	Masonry mortar	Joint mortar		sand	beige/brown	grey	Inc
S57	Republican Diana's Temple	TMP	I-II BC	Masonry mortar	Joint mortar		sand	beige/brown	grey	Inc
S50	Imperial forum basilica	FBI	I-III AD	Masonry mortar	Joint mortar		gravel	white/beige	grey	T

S58	Imperial forum basilica	FBI	I-III AD	Masonry mortar	Joint mortar	gravel	white/beige	grey	T
S55	Imperial forum basilica	FBI	I-III AD	Masonry mortar	Joint mortar	gravel	white/beige	grey	T
S3	Imperial forum basilica	FBI	I-III AD	Masonry mortar	Joint mortar	gravel	white/beige	grey	T
S51	Imperial forum basilica	FBI	?	Masonry mortar	Joint mortar	gravel	white/beige	grey	T
S49	Imperial forum tabernae	TFI	I-III AD	Masonry mortar	Joint mortar	gravel	white/beige	grey	T
S48	Imperial forum tabernae	TFI	I-III AD	Masonry mortar	Joint mortar	gravel	white/beige	grey	T
S52	Imperial forum Curia (wall)	CUR	I-III AD	Masonry mortar	Joint mortar	gravel	white/beige	grey	T
S56	Imperial forum Curia (pavement)	CUR	I-III AD	Masonry mortar	Joint mortar	gravel	white/beige	grey	T
S53	Imperial forum Curia (wall)	CUR	I-III AD	Masonry mortar	Joint mortar	gravel	white/beige	grey	T
S64	Theatre (proscaenium base)	TR	I-III AD	Masonry mortar	Joint mortar	sand	white	grey	T
S65	Theatre (proscaenium base)	TR	I-III AD	Masonry mortar	Joint mortar	sand	white	grey	T
S67	Theatre (valva regia)	TR	I-III AD	Masonry mortar	Joint mortar	sand	white	grey	T
S68	Theatre (western aditus)	TR	I-III AD	Masonry mortar	Joint mortar	sand	white	grey	T
S69	Theatre (western ima cavea)	TR	I-III AD	Masonry mortar	Joint mortar	sand	white	grey	T
S66	Theatre (western ima cavea)	TR	I-III AD	Masonry mortar	Joint mortar	sand	white	grey	T
S1	Islamic wall (1st track)	MI	VII-XII AD	Masonry mortar	Joint mortar	gravel	white/beige	grey	T
S39	Islamic wall (1st track)	MI	VII-XII AD	Masonry mortar	Joint mortar	gravel	white/beige	grey	T
S40	Islamic wall (1st track)	MI	VII-XII AD	Masonry mortar	Joint mortar	gravel	white/beige	grey	T
S17	Islamic wall (1st track)	MI	VII-XII AD	Masonry mortar	Joint mortar	gravel	white/beige	grey	T
S9	Islamic wall (2nd track)	MII	VII-XII AD	Masonry mortar	Joint mortar	gravel	white/beige	grey	T
S10	Islamic wall (2nd track)	MII	VII-XII AD	Masonry mortar	Joint mortar	gravel	white/beige	grey	T
S43	Islamic wall (2nd track)	MII	VII-XII AD	Masonry mortar	Joint mortar	gravel	white/beige	grey	T
S11	Islamic wall (2nd track)	MII	VII-XII AD	Masonry mortar	Joint mortar	gravel	white/beige	grey	T
S42	Islamic wall (2nd track)	MII	VII-XII AD	Masonry mortar	Joint mortar	gravel	white	grey	T
S2	Modern wall (16th cent.)	MXVI	XVI AD	Masonry mortar	Joint mortar	gravel	white	grey	T
S4	Hermitage (17th cent.)	ERM	XVII AD	Masonry mortar	Joint mortar	gravel	white	grey	T

S5	Napoleonic Household	DNAP	XIX AD	Masonry mortar	Joint mortar	gravel	white	grey	T

Table 1. Sample description including, name of the analyzed samples, location and acronym.

Note: Macroscopic features: 1 Gravel (over 2 mm); sand (between 2 mm and 0.063 mm); Silt (less than 0.063 mm); 2 Very Tough (not burst); Tenacious (breaks without breaking apart); Friable (crumble to finger pressure); Inconsistent (it is inconsistent to the touch).

ELEMENTS	NIM-GBW07408		NCS-DC60108a	
	Certified	Obtained	Certified	Obtained
Al_2O_3	11,92 ± 0,15	11,9 ± 0,5	0,33±0,03	0,4 ± 0,5
SiO_2	58,61 ± 0,13	58,2 ± 1,7	2,09±0,06	2,6 ± 0,3
CaO	8,27 ± 0,12	7,83 ± 0,09	51,61±0,15	51,2 ± 0,5
Ti	0,38 ± 0,01	0,38 ± 0,01	0,006 ± 0,002	< LOD
Fe	4,08 ± 0,07	4,071 ± 0,002	0,118±0,004	0,761 ± 0,004

Table 2. Accuracy of XRF analysis evaluated from the use of CRM (soil NIM-GBW07408 and limestone NCS DC60108a) reference samples. Note: Obtained values and certified values of the analyzed elements. Values expressed as percentage (%).

Vacuum pressure	5x$\mathbf{10}^{-5}$torr
Nebulizer Gas Flow	0.92 L/min
RF power	1100 Watts
Nebulizer pump	20 rpm
Tubes internal diameter	0,76 mm
Lens voltage	6.5-8.5 volts
Analog stage	-1950 volts
Pulse stage	1050 volts
Read Delay	15 sec
Sample flush	60 sec
Reading parameters	• Dwell Time UMA: 50ms • Sweeps: 20 • Readings: 1 • Replicates: 3

Table 3. ICP-MS employed parameters for mortar mineral element composition analysis.

ELEMENT	MASS [Da]	LOD	LOQ	R^2
La	139	0.0004	0.0014	0.9997
Ce	140	0.0005	0.0018	0.9997
Pr	141	0.00010	0.0003	0.9997
Nd	142	0.0003	0.0010	0.9985
Sm	152	0.0003	0.0011	0.9999
Eu	151	6E-05	0.00018	0.9998
Gd	158	0.00015	0.0005	0.9998
Tb	159	5E-05	0.00017	0.9977
Dy	162	1.1E-05	4E-05	0.9998
Ho	165	3E-05	0.00011	0.9983
Er	166	0.00013	0.0005	0.9999
Tm	169	1.6E-05	5E-05	0.9985
Yb	172	7E-05	0.0002	0.9999
Lu	175	1.7E-05	6 E-05	0.9991
Sc	45	0.013	0.04	0.9998
Y	89	0.0005	0.0016	0.9996
Sr	88	0.0012	0.004	0.9999
Tl	205	0.00008	0.003	0.9999
Zn	64	0.0015	0.005	0.9998
Cu	63	0.0014	0.004	0.9999
Ba	138	0.0010	0.003	0.9999
Mn	55	0.002	0.007	0.9997
Bi	209	0.0006	0.002	0.9999
Cd	111	0.00017	0.0006	0.9995
Cr	52	0.01	0.3	0.9986
Co	59	0.0004	0.0014	0.9986
Pb	207	0.0007	0.002	0.9996
Li	7	0.0002	0.0008	0.9994
Mo	95	0.0011	0.004	0.9998
Ni	60	0.007	0.02	0.9996
V	51	0.03	0.11	0.9999
Rh*	103			

Table 4. Analytical features of mortar sample ICP-MS analysis. Note: Mass, detection limits (LOD), quantification limits (LOQ) and R^2 of 31 elements detected in the studied samples being LOD and LOQ expressed as μg/g for all elements.*Internal Standard.

Acronym	Sample	Al_2O_3	SiO_2	CaO	Fe	Ti	Acronym	Sample	Al_2O_3	SiO_2	CaO	Fe	Ti
	S63	13.8	50.8	16.7	2.4	0.27		S49	0.5	15.0	41.0	1.1	0.10
	S7	12.8	51.2	14.5	2.2	0.28	TFI	S48	0.5	14.2	44.2	0.9	0.07
	S60	13.3	48.8	15.1	2.3	0.30		**Mean**	0.5	14.6	42.6	1.0	0.08
	S62	13.5	47.9	13.7	2.5	0.30		**SD**	0.0	0.6	2.3	0.1	0.02
	S41	12.4	46.7	15.0	2.5	0.27		S52	2.0	32.1	22.7	1.0	0.09
SMR	S6	13.5	46.5	15.3	2.6	0.29		S56	0.7	9.2	45.5	0.8	0.10
	S44	13.7	45.3	17.3	2.3	0.27	CUR	S53	0.9	19.4	35.4	1.4	0.15
	S8	13.3	44.4	16.4	2.5	0.30		**Mean**	1.2	20.3	34.5	1.1	0.11
	S61	13.3	46.7	15.4	2.4	0.29		**SD**	0.7	11.5	11.4	0.3	0.03
	S59	13.9	47.6	16.2	2.6	0.29		S64	0.4	20.7	37.9	1.0	0.09
	Mean	13.4	13.4	15.6	2.4	0.29		S65	0.5	17.7	35.5	1.1	0.09
	SD	0.5	2.2	1.1	0.1	0.01		S67	0.6	21.6	39.0	0.9	0.07
	S37	12.6	38.7	17.2	2.8	0.30	TR	S68	0.6	16.0	35.8	1.0	0.09
	S13	10.5	35.5	14.6	2.6	0.30		S69	0.4	18.6	38.1	0.8	0.06
	S16	12.3	38.7	15.3	2.3	0.28		S66	0.3	18.7	35.1	0.8	0.07
	S15	12.6	41.4	16.3	2.4	0.28		**Mean**	0.5	18.9	36.9	0.9	0.08
TCE	S38	11.2	39.4	20.2	2.0	0.23		**SD**	0.1	2.0	1.6	0.1	0.01
	S14	0.8	7.8	49.1	0.7	0.07		S1	0.5	12.3	44.2	0.7	0.07
	S12	0.6	12.3	48.4	0.9	0.08		S39	0.7	8.8	52.0	1.0	0.08
	Mean	8.6	30.5	25.9	2.0	0.22	MI	S40	0.9	12.8	37.5	1.0	0.10
	SD	5.5	14.2	15.8	0.8	0.10		S17	1.0	11.7	47.0	1.2	0.12
	S72	11.0	36.7	19.5	2.3	0.25		**Mean**	0.8	11.4	45.2	1.0	0.09
	S47	11.7	40.6	14.8	2.4	0.31		**SD**	0.2	1.8	6.0	0.2	0.02
FRW	S45	10.4	37.1	20.9	2.3	0.24		S9	0.8	14.7	40.2	1.2	0.12
	Mean	11.0	38.2	18.4	2.3	0.27		S10	0.8	12.9	40.4	1.1	0.10
	SD	0.6	2.2	3.2	0.1	0.04		S43	1.1	20.5	38.8	1.4	0.13
	S54	11.7	40.5	14.8	2.5	0.29	MII	S11	1.1	18.1	39.7	1.4	0.13
	S46	12.4	42.4	15.0	2.4	0.29		S42	0.7	8.3	48.4	0.9	0.06
TMP	S57	11.9	43.5	13.2	2.3	0.31		**Mean**	0.9	14.9	41.5	1.2	0.11
	Mean	12.0	42.1	14.3	2.4	0.30		**SD**	0.2	4.7	3.9	0.2	0.03
	SD	0.4	1.5	1.0	0.1	0.01	**MXVI***	S2	0.5	16.9	42.2	0.8	0.07
	S50	0.9	18.4	40.6	1.2	0.11	**ERM***	S4	0.4	20.1	36.3	1.1	0.08
	S58	0.8	15.5	35.0	1.5	0.14	**DNAP***	S5	0.6	15.9	35.7	1.2	0.08
	S55	0.6	15.7	38.3	1.7	0.12		**Mean**	0.5	17.6	38.0	1.1	0.08
FBI	S3	0.7	21.3	37.4	1.1	0.08		**SD**	0.1	2.2	3.6	0.2	0.01
	S51	0.5	14.8	38.9	1.1	0.08							
	Mean	0.7	17.1	38.0	1.3	0.10							
	SD	0.2	2.7	2.1	0.3	0.03							

Table 5. Chemical composition of samples from Sagunto Castle determined by PXRF.

Note: Concentration of elements expressed as percentage (%). Mean and standard deviation (SD) of the groups. * Samples belonging to modern buildings.

Acronym	Sample	REE	^{209}Bi	^{207}Pb	^{205}Tl	^{138}Ba	^{111}Cd	^{95}Mo	^{89}Y	^{88}Sr	^{64}Zn	^{63}Cu	^{60}Ni	^{59}Co	^{55}Mn	^{52}Cr	^{51}V	^{45}Sc	^{7}Li
SMR	**S63**	51	0.04	33	0.08	94	0.23	0.45	9.61	310	40	25	32	10	587	31	6.97	3.25	0.01
	S7	59	0.18	25	0.20	120	<LOD	0.31	6.48	201	17	12	20	7	406	19	0.39	3.97	26.49
	S60	53	0.003	15	0.09	106	0.03	0.03	8.82	270	15	13	27	10	616	14	<LOD	3.02	0.01
	S62	57	0.05	18	0.09	96	0.24	0.27	8.89	257	22	15	27	10	565	25	13.05	3.49	0.01
	S41	69	0.20	79	0.29	107	0.07	0.40	7.68	236	21	24	26	12	648	23	20.34	5.69	0.05
	S6	76	0.13	61	0.26	116	<LOD	0.38	8.49	228	22	23	27	11	505	23	3.56	5.18	40.20
	S44	62	0.06	48	0.20	95	0.04	0.23	7.64	278	21	18	25	10	561	19	5.61	4.63	0.04
	S8	57	0.11	68	0.19	103	<LOD	0.30	6.72	248	29	25	24	9	417	18	<LOD	3.95	34.03
	S61	52	0.03	33	0.09	87	0.15	0.27	8.93	336	35	26	28	11	585	18	0.16	3.27	0.01
	S59	55	0.08	41	0.11	88	0.20	0.46	9.03	306	34	28	30	13	642	19	5.83	3.61	0.01
	Mean	59	0.09	42	0.16	101	0.14	0.31	8.23	267	26	21	27	10	553	21	7	4.0	10
	SD	8	0.07	22	0.08	11	0.09	0.13	1.05	42	8	6	3	1	85	5	7	0.9	17
TCE	**S37**	52	0.16	64	0.45	89	0.29	0.78	6.33	217	47	28	28	10	641	19	5.79	4.74	0.09
	S13	56	0.05	55	0.20	106	0.07	0.68	9.15	387	46	38	34	13	682	27	17.60	6.35	48.51
	S16	50	0.23	60	0.20	109	0.08	1.00	7.71	401	42	27	31	10	576	28	26.87	5.80	40.86
	S15	46	0.06	51	0.15	86	0.01	0.28	8.19	359	39	28	34	12	648	23	4.46	4.97	40.11
	S38	43	0.20	86	0.38	93	0.54	0.59	4.98	276	25	22	21	8	401	14	0.11	3.90	0.07
	S14	31	0.02	21	0.06	85	<LOD	0.20	4.57	247	8	9	30	7	178	12	<LOD	2.70	12.65
	S12	33	0.02	8	0.07	100	<LOD	0.22	5.37	286	7	5	21	4	189	11	0.28	2.66	10.97
	Mean	44	0.10	49	0.21	95	0.2	0.5	6.61	310	31	22	28	9	473	19	9	4.4	22
	SD	10	0.09	27	0.15	10	0.2	0.3	1.76	72	17	11	6	3	218	7	11	1.4	21
FRW	**S72**	43	0.06	27	0.05	76	0.13	1.23	10.94	421	31	32	37	23	757	22	34.29	3.82	0.02
	S47	64	0.11	53	0.26	119	0.10	0.52	8.63	386	29	23	28	11	739	23	16.42	5.53	0.04
	S45	59	0.12	263	0.21	145	0.39	0.25	8.02	619	51	60	30	11	778	15	1.35	3.74	0.05
	Mean	55	0.10	115	0.18	113	0.2	0.7	9.20	476	37	38	32	15	758	20	17	4.37	0.04
	SD	11	0.03	129	0.11	35	0.2	0.5	1.54	126	12	19	5	7	20	5	16	1.01	0.02

TMP	**S54**	76	0.22	38	0.17	102	0.19	1.09	10.06	308	36	20	30	12	704	28	36.06	5.46	0.03
	S46	64	0.07	51	0.19	100	0.09	0.31	8.25	258	24	19	27	11	670	21	6.10	5.04	0.04
	S57	65	0.15	23	0.11	67	0.14	0.82	7.89	242	34	16	23	9	485	21	22.92	3.87	0.02
	Mean	68	0.15	37	0.16	90	0.14	0.7	8.73	269	31	19	27	11	620	23	22	4.8	0.03
	SD	7	0.07	14	0.05	20	0.05	0.4	1.16	34	6	2	4	1	118	4	15	0.8	0.01
FBI	**S50**	28	0.04	17	0.09	50	0.02	0.42	5.17	368	<LOD	11	22	6	430	7	2.48	1.95	0.01
	S58	28	0.04	35	0.08	77	0.08	0.41	5.50	732	32	15	27	8	465	10	2.42	2.26	0.01
	S55	26	0.04	7	0.07	58	0.09	1.31	5.40	597	<LOD	7	21	6	510	9	0.11	2.34	0.01
	S3	30	0.07	43	0.16	70	0.08	1.10	4.70	257	7	10	16	4	210	9	<LOD	2.33	15.93
	S51	24	0.01	12	0.08	54	0.01	0.36	5.11	399	<LOD	8	21	5	358	7	0.21	1.91	0.01
	Mean	27	0.04	23	0.10	62	0.06	0.7	5.18	470	20	10	21	6	395	8	1.3	2.2	3
	SD	2	0.02	15	0.04	12	0.04	0.4	0.31	191	18	3	4	1	117	2	1.3	0.2	7

Acronym	Sample	REE	^{209}Bi	^{207}Pb	^{205}Tl	^{138}Ba	^{111}Cd	^{95}Mo	^{89}Y	^{88}Sr	^{64}Zn	^{63}Cu	^{60}Ni	^{59}Co	^{55}Mn	^{52}Cr	^{51}V	^{45}Sc	^{7}Li
TFI	**S49**	34	0.06	22	0.11	82	0.09	0.22	6.19	479	7	10	24	5	335	11	7.87	2.71	0.01
	S48	30	0.07	27	0.13	91	0.22	0.47	6.13	731	12	16	22	5	474	8	9.68	2.35	0.02
	Mean	32	0.066	24	0.12	86	0.15	0.3	6.16	605	10	13	23	5	405	9	8.8	2.5	0.014
	SD	2	0.004	3	0.01	6	0.10	0.2	0.04	178	4	4	1.0	0.2	99	2	1.3	0.3	0.003
CUR	**S52**	24	0.06	18	0.07	49	0.18	0.40	5.87	326	3	8	19	3	267	5	0.00	1.70	0.005
	S56	29	0.09	65	0.13	80	0.05	0.61	3.16	656	12	187	28	7	234	9	19.27	1.99	0.01
	S53	31	0.11	40	0.10	72	0.14	0.42	5.70	656	29	19	24	6	436	11	9.79	2.31	0.01
	Mean	28	0.09	41	0.10	67	0.12	0.48	5	546	15	71	24	6	312	9	10	2.0	0.006
	SD	4	0.03	24	0.03	16	0.07	0.12	2	190	13	100	5	2	109	3	10	0.3	0.002
TR	**S64**	27	0.05	10	0.08	83	0.19	0.55	6.37	578	12	8	22	4	341	9	8.10	1.82	0.01
	S65	22	0.06	15	0.06	82	0.06	0.57	5.70	563	12	17	24	5	414	8	4.66	1.36	0.005

	S67	27	0.05	8	0.15	97	0.16	0.63	5.37	417	9	9	25	5	289	8	11.67	1.38	0.004
	S68	46	0.06	8	0.06	411	0.11	0.69	14.46	671	20	7	27	6	2454	10	17.02	3.68	0.01
	S69	22	0.03	9	0.04	157	0.13	1.94	8.19	1391	68	13	25	5	479	10	13.70	1.64	0.01
	S66	19	0.02	41	0.05	128	0.14	2.73	5.85	614	14	14	24	5	385	10	2.72	1.31	0.01
	Mean	27	0.05	15	0.07	160	0.13	1.2	8	706	23	12	24	5	727	9	10	1.9	0.007
	SD	10	0.01	13	0.04	127	0.04	0.9	3	346	22	4	2	1	849	1	5	0.9	0.002
MI	**S1**	25	0.11	9	0.32	101	0.08	0.49	3.49	204	6	6	19	4	185	7	<LOD	2.04	11.59
	S39	25	0.08	16	0.23	135	0.04	0.43	3.40	246	<LOD	6	21	6	199	8	<LOD	2.48	0.03
	S40	32	0.06	46	0.19	135	0.51	0.38	4.16	420	13	9	19	5	270	10	3.90	3.05	0.04
	S17	36	0.07	21	0.10	112	<LOD	0.36	5.51	359	14	12	30	7	275	18	9.68	4.19	18.23
	Mean	29	0.08	23	0.21	121	0.2	0.41	4.14	307	11	8	22	5	232	11	7	2.9	7
	SD	5	0.02	16	0.09	17	0.3	0.06	0.97	100	4	3	6	1	47	5	4	0.9	9
MII	**S9**	48	0.06	18	0.11	119	<LOD	0.52	6.06	414	15	7	19	5	231	13	<LOD	3.43	16.98
	S10	54	0.02	7	0.13	136	<LOD	0.46	7.16	375	11	6	22	8	233	16	1.44	4.21	22.26
	S43	48	0.09	21	0.18	139	0.13	0.37	6.21	384	9	11	21	8	479	15	16.42	4.25	0.02
	S11	47	0.02	21	0.10	169	0.03	0.21	6.51	422	6	8	25	7	333	14	<LOD	3.91	15.99
	S42	45	0.04	22	0.18	82	0.01	0.43	5.97	317	1	10	24	7	282	14	12.31	4.12	0.02
	Mean	48	0.05	18	0.14	129	0.06	0.40	6.4	382	8	8	22	7	312	14	10	4.0	11
	SD	3	0.03	6	0.04	32	0.07	0.12	0.5	42	5	2	2	1	103	1	8	0.3	10
MXVI ERM DNAP	**S2***	35	0.19	11	0.24	76	0.15	0.63	4.60	236	6	4	16	4	172	8	<LOD	2.36	13.79
	S4*	33	0.09	17	0.13	67	0.02	0.70	5.90	400	12	5	16	4	288	7	<LOD	2.36	17.74
	S5*	53	0.08	8	0.15	166	<LOD	1.10	8.06	212	2	6	16	4	643	14	<LOD	2.92	18.11
	Mean	40	0.12	12	0.17	103	0.08	0.8	6	283	7	5	16.0	3.9	368	10	-	2.5	17
	SD	11	0.06	4	0.06	55	0.09	0.3	2	102	5	1	0.2	0.4	246	4	-	0.3	2

Table 6. Chemical composition of mortar samples from Sagunto Castle determined by ICP-MS.

Note: Concentration of elements in μg/g. Mean and standard deviation (SD) of the groups. Total sum of Rare Earth Elements (REE). * Samples belonging to modern buildings.

Figure 1

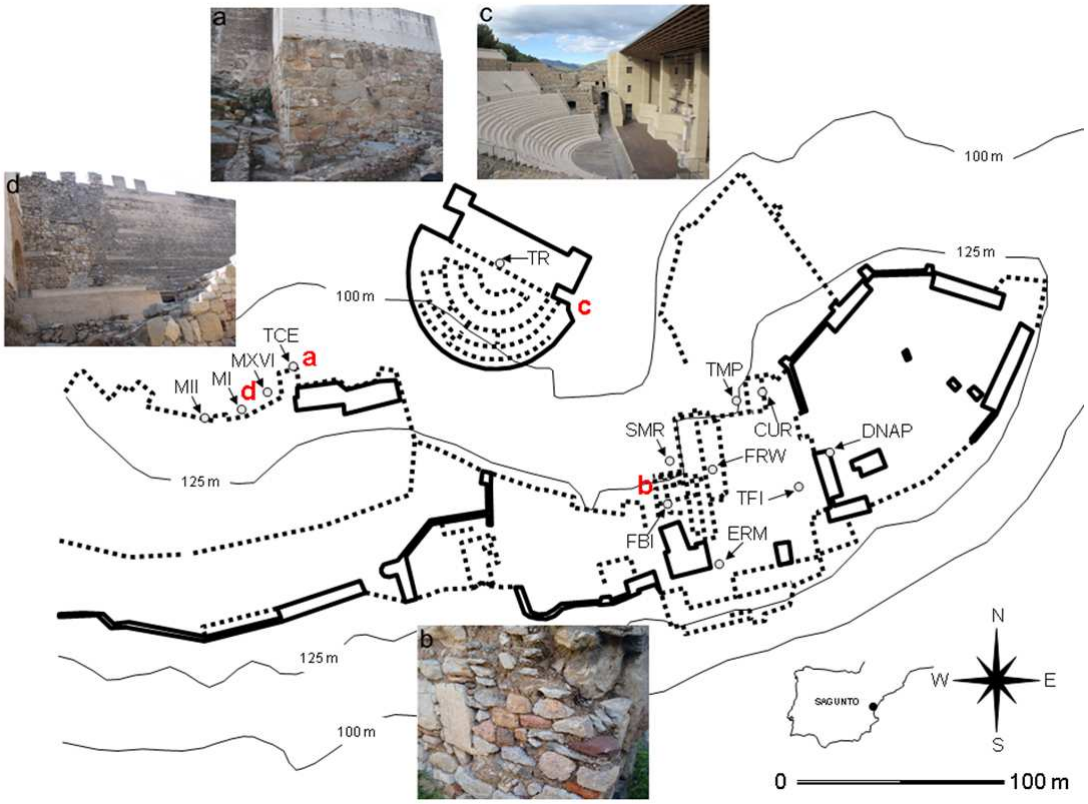
a
c
d
b
TR
c
100 m
125 m
TCE
MXVI
a
MII
MI
d
TMP
SMR
CUR
DNAP
FRW
b
TFI
FBI
ERM
125 m
100 m
N
W
E
S
SAGUNTO
0
100 m

Figure 2

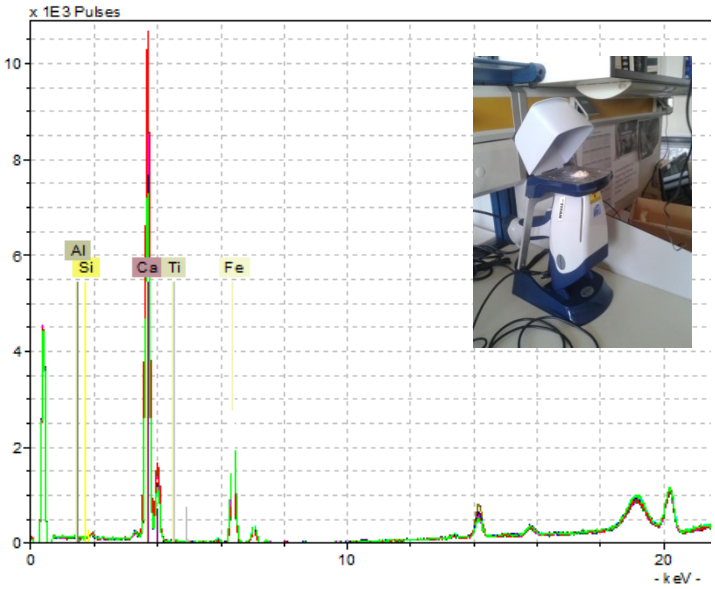

Figure 3

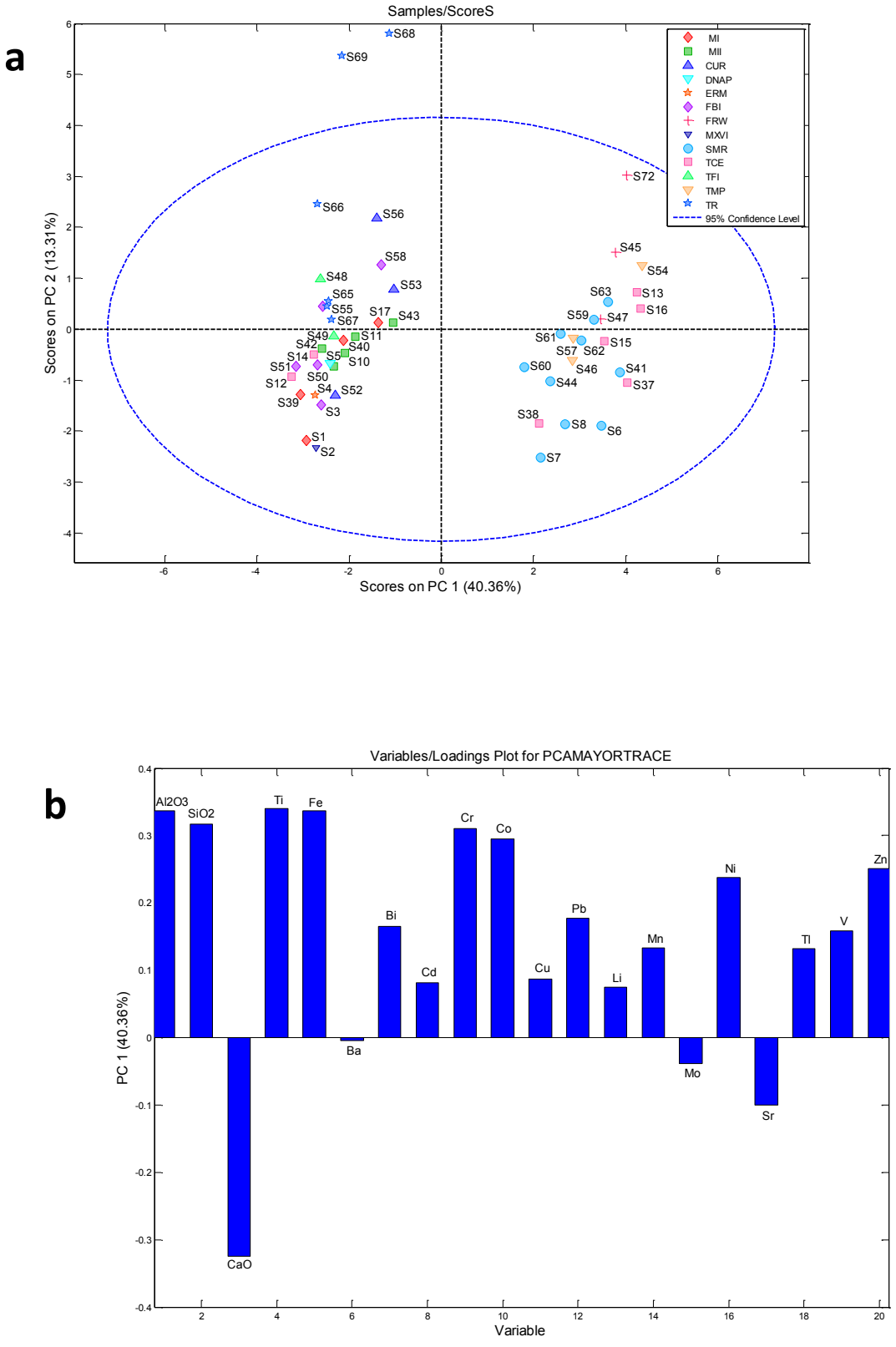
a
Samples/ScoreS
MI
MII
CUR
DNAP
ERM
FBI
FRW
MXVI
SMR
TCE
TFI
TMP
TR
95% Confidence Level
Scores on PC 2 (13.31%)
Scores on PC 1 (40.36%)
b
Variables/Loadings Plot for PCAMAYORTRACE
PC 1 (40.36%)
Variable
Al2O3
SiO2
CaO
Ti
Fe
Ba
Bi
Cd
Cr
Co
Cu
Pb
Li
Mn
Mo
Ni
Sr
Tl
V
Zn

Figure 4

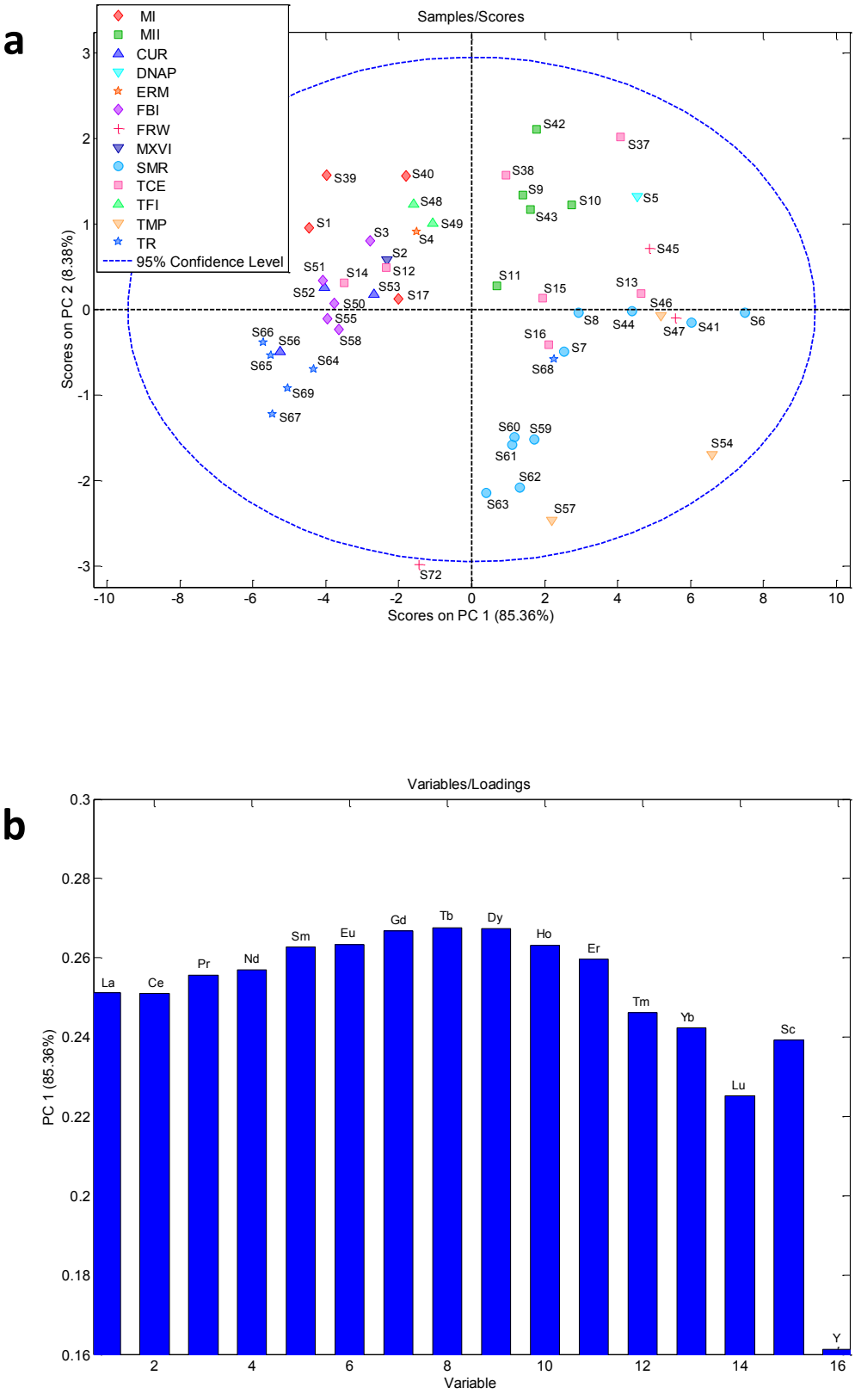
a
Samples/Scores
MI
MII
CUR
DNAP
ERM
FBI
FRW
MXVI
SMR
TCE
TFI
TMP
TR
95% Confidence Level
Scores on PC 2 (8.38%)
Scores on PC 1 (85.36%)
b
Variables/Loadings
PC 1 (85.36%)
Variable
La
Ce
Pr
Nd
Sm
Eu
Gd
Tb
Dy
Ho
Er
Tm
Yb
Lu
Sc
Y

Figure 5

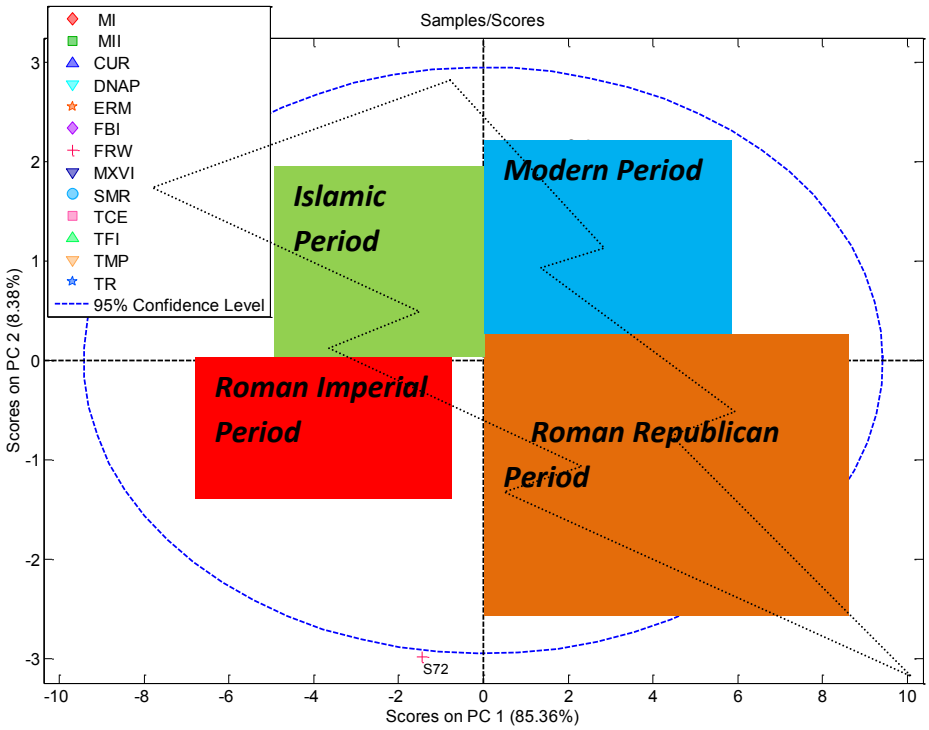
Samples/Scores
MI
MII
CUR
DNAP
ERM
FBI
FRW
MXVI
SMR
TCE
TFI
TMP
TR
95% Confidence Level
Islamic Period
Modern Period
Roman Imperial Period
Roman Republican Period
S72
Scores on PC 2 (8.38%)
Scores on PC 1 (85.36%)
3
2
1
0
-1
-2
-3
-10
-8
-6
-4
-2
0
2
4
6
8
10